The Internal Dynamic Modes of Charged Self-Assembled Peptide Fibrils

ARTICLE *in* LANGMUIR · MAY 2005

Impact Factor: 4.46 · DOI: 10.1021/la046802f · Source: PubMed

9 AUTHORS, INCLUDING:

Manlio Tassieri
University of Glasgow
40 PUBLICATIONS **444** CITATIONS
SEE PROFILE

Amalia Aggeli
University of Leeds
77 PUBLICATIONS **3,100** CITATIONS
SEE PROFILE

Neville Boden
University of Leeds
87 PUBLICATIONS **3,201** CITATIONS
SEE PROFILE

John Fisher
University of Leeds
580 PUBLICATIONS **14,315** CITATIONS
SEE PROFILE

The Internal Dynamic Modes of Charged Self-Assembled Peptide Fibrils

L. Carrick,[†] M. Tassieri,[‡] T. A. Waigh,*[,‡] A. Aggeli,[†] N. Boden,[†] C. Bell,[§] J. Fisher,[§] E. Ingham,[||] and R. M. L. Evans[‡]

Centre for Self-Organising Molecular Systems, Department of Chemistry, University of Leeds, Leeds LS2 9JT, U.K., Polymers and Complex Fluids, Department of Physics and Astronomy, University of Leeds, Leeds LS2 9JT, U.K., Department of Mechanical Engineering, University of Leeds, Leeds LS2 9JT, U.K., and Department of Biochemistry and Microbiology, University of Leeds, Leeds LS2 9JT, U.K.

Received December 23, 2004. In Final Form: March 7, 2005

Photon correlation spectroscopy is used to study the internal dynamics of self-assembled charged peptide fibrils. Short neutral and charged polymeric aggregates have diffusive modes due to whole macromolecular motion. For long semiflexible fibrils the logarithm of the intermediate scattering function follows a $q^2t^{3/4}$ scaling at long times consistent with a Kratky−Porod free energy and preaveraged Oseen hydrodynamics. Persistence lengths on the order of micrometers are calculated for the peptide fibrils consistent with estimates from the liquid-crystalline phase behavior. Fibril diameters (5−35 nm) calculated from the initial decay of the correlation functions are in agreement with transmission electron microscopy measurements.

Molecular self-assembly has been the topic of intense scientific investigations in recent years due to a necessity to understand biological molecular self-assembly, as well as self-assembly of pathological structures such as amyloid fibrils, e.g., in Alzheimer's disease.[1,2] Moreover molecular self-assembly is believed to be one of the main routes for the production of well-defined functional nanostructures for applications in nanotechnology. Peptides have an intrinsic propensity for self-assembly. Learning to control it can lead to a wealth of versatile peptide-based self-assembled nanostructures whose properties can be engineered by appropriate peptide design to match the requirements of specific applications such as artificial boundary lubricants in articulated joints or for tissue scaffolding.

The biological beta-sheet motif has been exploited to design peptides that self-assemble in one dimension into a hierarchy of well-defined elongated structures such as tapes (single molecule in thickness), ribbons (a pair of stacked tapes), fibrils (several stacked and twisted ribbons), and fibers (a pair of entwined fibrils).[1,2] All these structures are twisted due to the inherent chirality of the peptide molecules. At high enough concentration in solution these aggregates give rise to organogels, hydrogels, or nematic fluids and gels. Traditional high-resolution structural techniques such as X-ray crystallography and high-resolution solution NMR cannot be applied to these aggregates. Therefore there is the need to use a range of other complementary techniques to build a precise picture of the structure and properties of these aggregates at high resolution and to establish in a quantitative manner how they vary by systematic changes of the molecular structure and solution conditions. This will lead to a better understanding of biological peptide self-assembly and an increased ability to design peptidic systems with a combination of desirable properties for nanotechnology.

The physical properties of the peptide materials studied are sensitively related to the charge fraction,[3] the chirality, and the interpeptide energy. There is a complicated variety of physical interactions which occur in self-assembling peptides. Theoretical studies specifically applied to the current peptide fibrils have examined the self-assembly of the materials, the liquid crystalline phases, and the effect of chirality on the resultant fibril morphology.[4,5]

Actin, whose polymeric aggregates have many features in common with the current peptide system, is the most extensively studied self-assembled semiflexible polymer.[6] This is mainly due to its importance in naturally occurring motor protein systems, since purification of the proteins can be challenging. Over 50 naturally occurring proteins are known to bind to actin.[7] The dynamic modes have been measured with dynamic light scattering,[8] and a distinctive spectrum of internal flexural modes is observed due to transverse fluctuations of the chains.[6] Similarly the high-frequency viscoelastic modes are distinctive (shear moduli G', $G'' \propto \omega^{3/4}$) as measured with microrheology techniques, such as diffusing wave spectroscopy and laser tracking,[9] and agree well with theory.[10] The *de novo*

* To whom correspondence should be addressed. E-mail: t.a.waigh@leeds.ac.uk.

[†] Centre for Self-Organising Molecular Systems, Department of Chemistry.

[‡] Polymers and Complex Fluids, Department of Physics and Astronomy.

[§] Department of Mechanical Engineering.

[||] Department of Biochemistry and Microbiology.

(1) Aggeli, A.; Nyrkova, I. A.; Bell, M.; Harding, R.; Carrick, L.; McLeish, T. C. B.; Semenov, A. N.; Boden, N. Hierarchical self-assembly of chiral rodlike molecules as a model for peptide beta-sheet tapes, ribbons, fibrils, and fibers. *Proc. Natl. Acad. Sci. U.S.A.* **2001**, *98* (21), 11857−11862.

(2) Aggeli, A.; Bell, M.; Boden, N.; Keen, J. N.; Knowles, P. F.; McLeish, T. C. B.; Pitkeathy, M.; Radford, S. E. *Nature* **1997**, *386*, 259−262.

(3) Aggeli, A.; Bell, M.; Carrick, L.; Fishwick, C. W. G.; Harding, R.; Mawer, P. J.; Radford, S. E.; Strong, A. E.; Boden, N. *J. Am. Chem. Soc.* **2003**, *125* (32), 9619−9628.

(4) Nyrkova, I. A.; Semenov, A. N.; Aggeli, A.; Bell, M.; Boden, N.; McLeish, T. C. B. *Eur. Phys. J. B* **2000**, *17*, 499−513.

(5) Nyrkova, I. A.; Semenov, A. N.; Aggeli, A.; Boden, N. *Eur. Phys. J. B* **2000**, *17*, 481−497.

(6) Farge, E.; Maggs, A. C. Dynamic scattering from semi-flexible polymers. *Macromolecules* **1993**, *26*, 5041−5044.

(7) Bray, D. *Cell Movements*; Garland: New York, 1992.

(8) Gotter, R.; Kroy, K.; Frey, E.; Barmann, M.; Sackmann, E. Dynamic light scattering from semidilute actin solutions: A study of hydrodynamic screening, filament bending stiffness, and the effect of tropomyosin/troponin-binding. *Macromolecules* **1996**, *29*, 30−36.

10.1021/la046802f CCC: $30.25
Published on Web 03/24/2005

Table 1. Peptide Sequences[a]

P_{11}-2	CH_3CO-Gln-Gln-Arg^+-Phe-Gln-Trp-Gln-Phe-Glu^--Gln-Gln-NH_2
P_{11}−3	CH_3CO-Gln-Gln-Arg^+-Phe-Gln-Trp-Gln-Phe-Gln-Gln-Gln-NH_2
P_{11}−4	CH_3CO-Gln-Gln-Arg^+-Phe-Glu^--Trp-Glu^--Phe-Glu^--Gln-Gln-NH_2
P_{11}−7	CH_3CO-Ser-Ser-Arg^+-Phe-Ser-Trp-Ser-Phe-Glu^--Ser-Ser-NH_2

[a] The underlining indicates differences in amino acid sequences compared to P_{11}-2.

Table 2. DLS and TEM Analysis of the Structure of the Self-Assembling Peptides

sample	concn (mM)	a (nm)	L_p (μm)	D (10^8 cm^2/s)	R_h (nm)	width (nm) (TEM)	c_{tape}* (mM) (CD[1])	peptide charge fraction
P_{11}-2 in water	0.31			1.30 ± 0.02	166 ± 2	10 ± 2	0.05	0
	0.63	34.5 ± 0.2	10 ± 3			10 ± 2		+1
	1.57	9 ± 3	6.4 ± 0.4			10 ± 3		+1
	3.14	8 ± 3	4.3 ± 0.5			10 ± 3		+1
	6.28	7 ± 1	3.4 ± 0.6			11 ± 2		+1
P_{11}-3 in water	0.31			1.2 ± 0.1	181 ± 9	5 ± 1	0.030	+1
	0.63			1.66 ± 0.03	131 ± 1	10 ± 2		
	1.57			3.9 ± 0.1	56 ± 0.8	9 ± 2		
	3.13			2.45 ± 0.04	88 ± 0.8	11 ± 1		
P_{11}-4 at pH 2	0.63	33.4 ± 1	2.2 ± 0.6			21 ± 13	0.012	+1
P_{11}-7 in water	0.74	4.7 ± 0.6	4.3 ± 0.6			6 ± 3	0.100	+1

peptide system we have examined in the present article has a number of advantages over actin, including the ability to vary the charge fraction by specific design of the peptide chemistry and the ease of sample purification.

Previous dynamic light scattering studies with self-assembled peptides have examined relatively flexible tapes (persistence length ~100 nm) in organic solvents and were thus not sensitive to the internal dynamics of the polymers.[11] In the present study we consider extremely long (several micrometers in length from transmission electron microscopy (TEM) measurements) charged peptide fibrils in aqueous solutions. We can thus probe the internal dynamics of the polymers with optical wavelengths (488 nm) and demonstrate the hydrodynamic signature of semiflexibility ($q^2t^{3/4}$ scaling of intermediate scattering function[6]) only previously seen with actin.

Gelling charged peptide (P_{11}-4) has been previously examined using small-angle neutron scattering in deuterated water.[12] The orientation and morphology under shear have been measured. Nematic phases of the self-assembled fibrils were clearly observed at the molecular level, and the diameter of the fibrils was calculated (8 nm).[12] For the phase diagram of the present materials we refer the reader to Aggeli et al.[3] and we build on these results in the present article.

In the current article we consider the self-assembled aggregates of a family of four peptides, all with 0−1 charge fraction per monomer at the chosen pH values. The charge needs to be limited, or the process of self-assembly is inhibited.[3] Changes in the sequence of the hydrophobicity/hydrophilicity and charge of the amino acids sensitively affect the resultant fibrillar length, width, and aggregation state.[13] The length of the peptide assemblies is directly reflected in the type of motion observed in DLS. Free translational diffusion is measured for short tapes, and semiflexible internal motions are measured with giant fibrils.

Experimental Section

Peptide Synthesis. Peptides P_{11}-2, P_{11}-3, P_{11}-7, and P_{11}-4 were purchased from NeoMPS Groupe SNPE (Strasbourg, France) (FW: 1593.6, 1592.6, 1347.3, and 1595.7 Da, respectively). P_{11}-4 was also purchased from SynPep (Dublin, CA). The primary structure of the peptides is described in Table 1. All peptides were prepared using standard solid phase Fmoc chemistry and purified by reversed-phase high-performance chromatography as described previously.[3] The degree of self-assembly and the resultant tape/ribbon/fibril/fiber morphology depends sensitively on the chemistry of the materials and the solution conditions.[1] The charge fraction of monomers (the average charge on a monomer) in the fibrils with the buffer pHs used are all in the range 0−1.

Sample Preparation for Dynamic Light Scattering. Solutions of P_{11}-2, -3, and -7 were prepared by the dissolution of lyophilized peptide in 18.2 MΩ water. A solution of P_{11}-4 at 0.63 mM peptide concentration was prepared by the dissolution of lyophilized peptide in phosphoric acid at pH 2. The water/buffer was prefiltered each time twice through a sterile 0.02 μm syringe filter. The solutions were sonicated for 10 min and stored at room temperature for a week.

Optical micrographs were recorded using an Olympus BH 2 light microscope fitted with an Olympus SC35 camera. Images were taken viewed through crossed-polarizers.

Transmission electron microscopy images were collected using a Philips CM 10 TEM at 80 kV accelerating voltage as described previously.[1−3] The peptide solutions were diluted to a peptide concentration of 20 μM using water or phosphoric acid at pH 2, and a drop applied to an ionized, carbon-coated copper grid for 60 s. A droplet of 4% uranyl acetate (negative stain) was applied to the grid for 20 s, and the grid was left to dry on filter paper.

Dynamic light scattering experiments were performed on a compact ALV500 goniometer using a fast correlator (>10 ns). A 100 mW argon ion laser was used as a coherent light source (488 nm wavelength). Correlation functions were measured over angles in the range 30−140°.

Results and Discussion

The self-assembly behavior of P_{11}-2 has been described in detail previously.[1] The critical concentration (c_{tape}*) for the onset of self-assembly of P_{11}-2 in water has been demonstrated with circular dichroism spectroscopy[1] to be 50 μM. A series of self-assembled morphologies form as the peptide monomer concentration is increased: mono-

(9) Schnurr, B.; Gittes, F.; MacKintosh, F. C.; Schmidt, C. F. Determining microscopic viscoelasticity in flexible and semiflexible polymer networks from thermal fluctuations. *Macromolecules* **1997**, *30*, 7781−7792.

(10) Xu, J.; Palmer, A.; Wirtz, D. Rheology and Microrheology of Semiflexible Polymer Solutions: Actin Filament Networks. *Macromolecules* **1998**, *31* (19), 6486−6492.

(11) Aggeli, A.; Fytas, G.; Vlassopoulos, D.; McLeish, T. C. B.; Mawer, P. J.; Boden, N. *Biomacromolecules* **2001**, *2* (2), 378−388.

(12) Mawer, P. J.; Waigh, T. A.; Harding, R.; McLeish, T. C. B.; King, S. M.; Bell, M.; Boden, N. Small-angle neutron scattering from peptide nematic fluids and hydrogels under shear. *Langmuir* **2003**, *19*, 4940−4949.

(13) Aggeli, A.; Bell, M.; Boden, N.; Carrick, L.; Strong, A. E. *Angew. Chem., Int. Ed.* **2003**, *42*, 5603−5606.

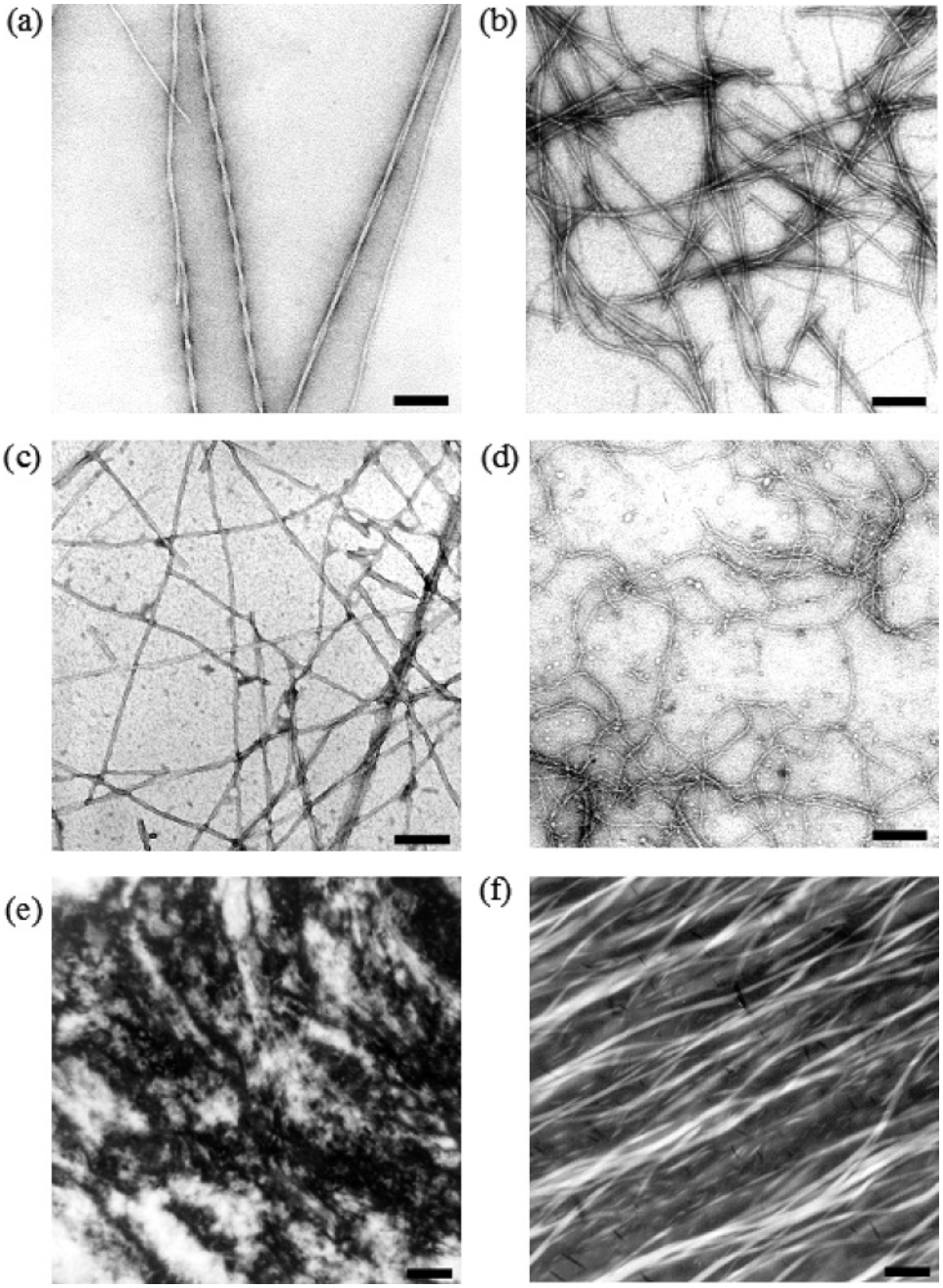

Figure 1. TEM images of (a) P_{11}-2 at 0.63 mM in water, (b) P_{11}-3 at 0.63 mM in water, (c) P_{11}-4 at 0.63 mM at pH 2 in H_3PO_4, and (d) P_{11}-7 at 0.74 mM in water (scale bars are 100 nm). Optical micrographs between crossed polarizers showing nematic phases of (e) P_{11}-2 at 6.3 mM in water and (f) P_{11}-3 at 3.13 mM in water (scale bars are 250 μm).

mers, tapes, ribbons, fibrils, and fibers.[1] Similar behavior is observed for the other peptides examined.

Nematic phases are observed at high concentrations with all the samples in optical microscopy and small-angle neutron scattering due to the rigidity and extremely high aspect ratio of the fibril morphology. Isotropic/nematic transitions were observed at 0.9, 0.63, 1.3, and 1.5 mM concentrations for P_{11}-2, P_{11}-3, P_{11}-4, and P_{11}-7, respectively, with optical microscopy. Evidence from TEM micrographs on the diameter is included in Table 2. No direct evidence for cross-links was found in the concentrations examined. An order of magnitude calculation of the persistence length (L_p) is provided by the Onsager formula for the volume fraction (Φ_{IN}) of the isotropic/nematic phase transition, $\Phi_{IN} = 5.51a_{eff}/L_p$, where a_{eff} is the effective diameter of the fibers including electrostatics.[12] This gives an order of magnitude value for L_p of 10 μm for P_{11}-2.

Correlation functions from DLS were initially examined with CONTIN (a numerical inverse Laplace transform algorithm) to detect the presence of diffusive motion in the samples. An example of free translational diffusive motion (relaxation rate (Γ) $\propto q^2$, correlation function $\propto t$) for P_{11}-3 is shown in Figure 2, q is the momentum transfer ($q = (4\pi n/\lambda)\sin(\theta/2)$, where λ is the wavelength, θ is the scattering angle, and n is the refractive index) and t is the time. Clearly there is a barrier to these peptides forming giant polymers and only short tapes are obtained. The diffusion coefficient (D) and hydrodynamic radii of gyration (R_h) obtained from the Stokes−Einstein relationship are collected in Table 2. For all of the samples examined, the correlation functions were found to be ergodic; i.e., the

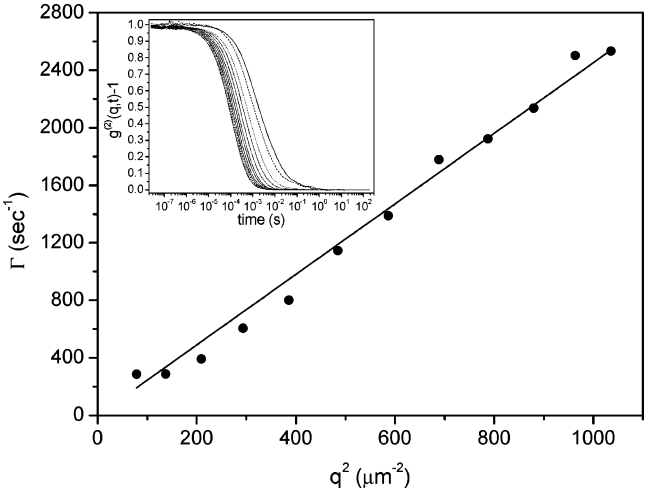

Figure 2. Diffusive dynamics of P_{11}-3 tapes at 3.13 mM are observed with a linear dependence of the decay rate (Γ) versus q^2 from DLS. The continuous line is a line of best fit. The inset shows the ergodic intensity correlation function from P_{11}-3 at a series of different angles (30−140°).

correlation functions decayed to zero at large times indicating the materials are weak gels or semidilute fluids as expected from TEM images.

For the giant fibrils that do not demonstrate free translational diffusive motion, the dynamic light scattering was examined separately in both the short and long time regimes. The initial short time decay was fitted with a single exponential, and the relaxation rates obtained (γ^0) were rescaled against q^3 (γ^0/q^3) and plotted against q to observe deviations from flexible Zimm behavior ($\Gamma \propto q^3$), Figure 3. Subsequently from the theory of Kroy and Frey assuming a Kratky−Porod free energy and preaveraged Oseen hydrodynamics, the hydrodynamic diameter of the fibril can be calculated[14]

$$g^{(1)}(q,t) = g^{(1)}(q,0)\exp(-\gamma^0 t) \tag{1}$$

$g^{(1)}(q,t)$ is the intermediate scattering function and $g^{(1)}(q,0)$ is the zero time intercept

$$\gamma^0 = \frac{k_B T}{6\pi^2 \eta_s} q^3 \left(\frac{5}{6} - \ln(qa)\right) \tag{2}$$

where $k_B T$ is the thermal energy, η_s is the solvent viscosity, and a is the hydrodynamic diameter of the fibril. Values of the hydrodynamic diameter calculated with fits to eq 2 (Figure 3) are included in Table 2. At long times the prediction is

$$g^{(1)}(q,t) = g^{(1)}(q,0)\exp\left(-\frac{\Gamma(1/4)}{3\pi}(\gamma_q t)^{3/4}\right) \tag{3}$$

where Γ(1/4) is the gamma function evaluated at 1/4

$$\gamma_q = \frac{k_B T q^{8/3}}{4\pi\eta_s L_p^{1/3}}\left(\frac{5}{6} - \ln(qa)\right) \tag{4}$$

The length scales in the experiment follow the inequalities $a \ll \lambda < \xi \ll L_P$, and $a \ll \lambda < \xi \ll L$. L is the contour length and ξ is the mesh size. The mesh size was estimated from electron microscopy images. Such separation of length scales is required for application of the theory.[6]

(14) Kroy, K.; Frey, E. *Phys. Rev. E* **1996**, *55*, 3092.

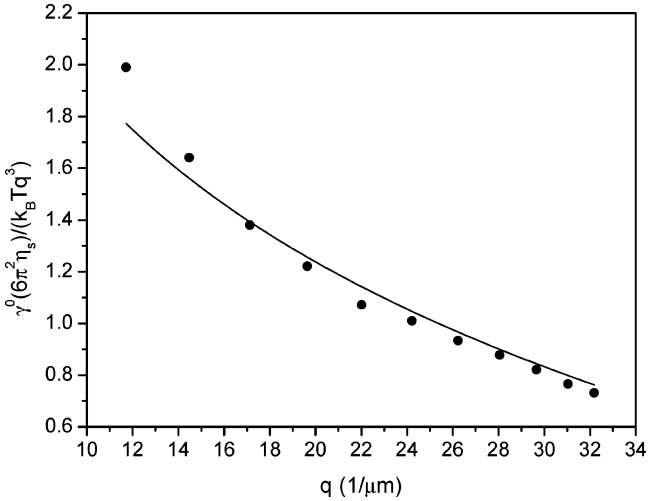

Figure 3. The initial decay rate (γ^0) of the intermediate scattering function of P_{11}-4 fibrils at 0.63 mM plotted as $\gamma^0(6\pi^2\eta_s)/(k_B T q^3)$ versus q. The semiflexible hydrodynamic corrections are seen in deviations from linearity, and a fit is shown to eq 2 (continuous line). The hydrodynamic diameters calculated are shown in Table 2.

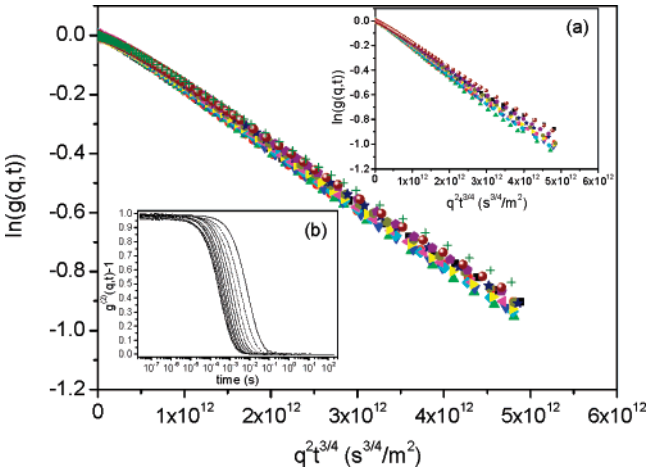

Figure 4. Long time decay of the correlation functions of P_{11}-4 fibrils at 0.63 mM from DLS showing universal $\exp(-q^2t^{3/4})$ behavior. A series of curves with separate q values all superpose (angles in the range 30−140°). Inset a shows similar behavior from P_{11}-2 fibrils at 0.63 mM. Inset b shows the ergodic intensity correlation functions of P_{11}-4 fibrils.

The prediction for the long time correlation of semiflexible polymers follows a universal $\exp(-q^2t^{3/4})$ scaling. We thus make a master plot of the data in this form, since it provides a sensitive test of the peptide dynamics (Figure 4). Analogously fitting $\ln(-\ln(g^{(1)}(q,t)/g^{(1)}(q,0))$ versus $\ln(t)$ provides an exponent β of 0.73, 0.75, and 0.63 for P_{11}-2, P_{11}-4, and P_{11}-7, respectively. However the short ribbon peptide P_{11}-3 clearly departs from such a stretched exponential scaling (Figure 2).

P_{11}-2 and P_{11}-4 follow the universal scaling of $\exp(-q^\alpha t^\beta)$ with $\alpha = 1.99 \pm 0.09$, 1.99 ± 0.02 and $\beta = 0.731 \pm 0.004$, 0.749 ± 0.005, respectively, giving strong evidence for the predicted stretched exponential behavior due to semiflexibility (prediction is $\alpha = 2$, $\beta = 3/4$) (Figure 4). These polymers demonstrate very good agreement with semiflexible polymer theory.[6] P_{11}-7 continues to have stretched exponential dynamics, but with weakened exponents for $\alpha = 1.88 \pm 0.06$ and $\beta = 0.629 \pm 0.005$. P_{11}-3 and P_{11}-2 at lower concentrations have no such scaling; there is a q^2 behavior of the relaxation rate (Figure 2). The cross over between the two behaviors, short peptide

tapes dominated by whole chain diffusion and giant semiflexible fibrils with distinctive internal modes, is in agreement with the numerical studies of Winkler et al.[15]

The persistence length of P_{11}-4 and P_{11}-7 is lower, but of the same order of magnitude as P_{11}-2, Table 2. Weak dependencies of the persistence length and diameter were observed with peptide concentration, but care should be taken with overinterpretation, since both self-assembly and interparticle interference affect the scattering functions.

The calculated hydrodynamic diameters of the fibrils from DLS are in fair agreement with estimates from TEM, Table 2, although the in situ DLS measurements are expected to be more accurate than those from dehydrated TEM samples. Depolarized light scattering measurements indicate a very slow rotational diffusion process occurs as expected for the entangled giant peptide fibrils. Further particle tracking microrheology and diffusing wave spectroscopy experiments indicate dynamical features consistent with semiflexibility and will be examined in future work.

Acknowledgment. We thank the EPSRC and the Royal Society for funding this research.

LA046802F

(15) Harnau, L.; Winkler, R. G.; Reineker, P. *J. Chem. Phys.* **1996**, *104* (16), 6355−6368.